

# **Addition Spectra of Quantum Dots: the Role of Dielectric Mismatch**

**A. Franceschetti,\* A. Williamson, and A. Zunger**

*National Renewable Energy Laboratory, Golden, Colorado 80401*

*Received: January 4, 2000; In Final Form: February 20, 2000*

Using atomistic pseudopotential wave functions, we calculate the electron and hole addition energies and the quasi-particle gap of InAs quantum dots. We find that the addition energies and the quasi-particle gap depend strongly on the dielectric constant  $\epsilon_{\text{out}}$  of the surrounding material, and that when

at infinite distance from the first dot). The energy required by this process (“quasi-particle gap”) is the difference between the ionization potential and the electron affinity of the dot. The initial configuration, consisting of the two neutral dots in the ground state, has energy  $2E_0$ , while the final configuration has energy  $E_1 + E_{-1}$ , where  $E_{-1}$  is the energy of the quantum dot with a hole in the highest occupied orbital h1. The quasi-particle gap is then

where  $\epsilon_{\text{gap}} = \epsilon_{\text{e1}} - \epsilon_{\text{h1}}$  is the single-particle (HOMO–LUMO)

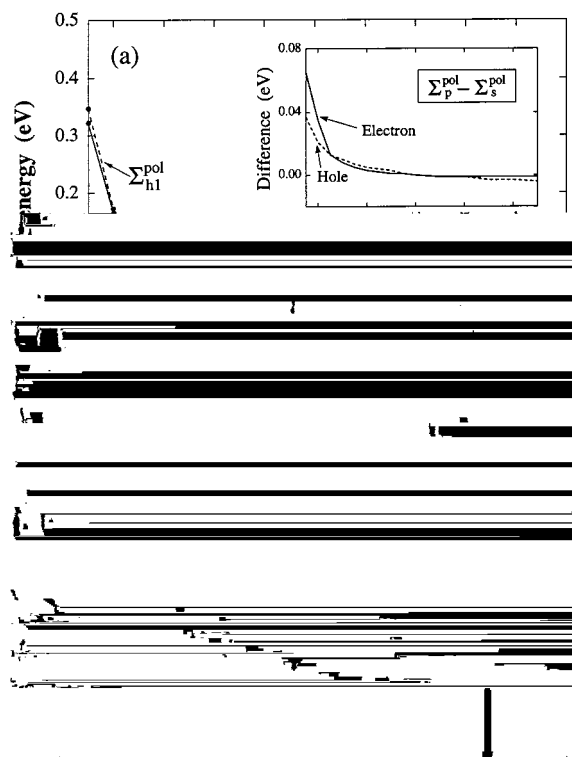


**Figure 2.** Self-energies  $\Sigma_i^{\text{pol}}$  and  $\Sigma_{e1}^{\text{pol}}$  (a) and polarization energies  $J_{h1,h1}^{\text{pol}}$  and  $J_{e1,e1}^{\text{pol}}$  (b) of an InAs quantum dot (diameter  $D = 30.3 \text{ \AA}$ ) shown as a function of the outside dielectric constant  $\epsilon_{\text{out}}$ . Also shown in (b) are the direct Coulomb energies  $J_{h1,h1}^{\text{dir}}$  and  $J_{e1,e1}^{\text{dir}}$ . The insets show the differences  $\Sigma_p^{\text{pol}} - \Sigma_s^{\text{pol}}$  and  $J_{sp}^{\text{pol}} - J_{ss}^{\text{pol}}$  as a function of  $\epsilon_{\text{out}}$ . The vertical arrows indicate the value  $\epsilon_{\text{out}} = \epsilon_{\text{in}}$ .

We see that (i) both  $\Sigma_i^{\text{pol}}$  and  $J_{ij}^{\text{pol}}$  depend strongly on  $\epsilon_{\text{out}}$  and vanish when  $\epsilon_{\text{out}} = \epsilon_{\text{in}}$  (vertical arrows in Figure 2); (ii) when  $\epsilon_{\text{out}} > \epsilon_{\text{in}}$  the polarization energies  $J_{ij}^{\text{pol}}$  become negative, thus acting to diminish the electron–electron interaction; (iii) the dependence of  $\Sigma_i^{\text{pol}}$  and  $J_{ij}^{\text{pol}}$  on the identity of the orbitals  $i$  and  $j$  (e.g., s or p) is rather weak, as shown in the insets in Figure

2; (iv) there is a critical value of  $\epsilon_{\text{out}}$  ( $\epsilon_{\text{critical}} \approx 4$ ) such that for  $\epsilon_{\text{out}} < \epsilon_{\text{critical}}$  the polarization energies  $J_{ij}^{\text{pol}}$  dominate over the direct Coulomb energies  $J_{ij}^{\text{dir}}$ .

The charging energies  $I_N = E_N - E_{N-1}$ , calculated from the total energies  $E_N$  given by eq 7, are shown in the central panel of Figure 3 as a function of  $\epsilon_{\text{out}}$ . The vertical arrow at the bottom of the figure denotes the value  $\epsilon_{\text{out}} = \epsilon_{\text{in}}$ , which divides the behavior into two domains: (i) In the weak screening regime ( $\epsilon_{\text{out}} \ll \epsilon_{\text{in}}$ ) the charging energies are widely spaced, and their value depends strongly on  $\epsilon_{\text{out}}$ . (ii) In the strong screening regime ( $\epsilon_{\text{out}} \geq \epsilon_{\text{in}}$ ) the charging energies are closely spaced and do not depend significantly on  $\epsilon_{\text{out}}$ . The calculated charging spectrum is shown in Figure 3 for  $\epsilon_{\text{out}} = 1$  (left-hand side) and  $\epsilon_{\text{out}} = 20$  (right-hand side), illustrating these two limiting behaviors.

The electron and hole addition energies  $\Delta_{N,N+1}$  (spacings between peaks in the charging spectra of Figure 3), the quasi-particle gap  $\epsilon_{\text{gap}}^{\text{qp}}$ , and the optical gap  $\epsilon_{\text{gap}}^{\text{opt}}$  are summarized in Table 1 for a few values of  $\epsilon_{\text{out}}$ .

**Electron Addition Energies.** We see from Table 1 that the addition energy of the third electron  $\Delta_{2,3}^{(e)}$  is significantly larger than the addition energy of the second electron  $\Delta_{1,2}^{(e)}$ . This can be explained by noting from eqs 4 and 5 that while  $\Delta_{1,2}^{(e)}$  measures only the interelectronic repulsion,  $\Delta_{2,3}^{(e)}$  includes also the single-particle gap  $\epsilon_{e2} - \epsilon_{e1}$  between the s-like state e1 and the p-like states e2, e3, and e4. We find  $\epsilon_{e2} - \epsilon_{e1} = 400 \text{ meV}$  for the  $30.3 \text{ \AA}$  diameter nanocrystal and  $360 \text{ meV}$  for the  $42.2 \text{ \AA}$  diameter nanocrystal. The addition energies of the remaining electrons (up to  $N = 8$ ) are approximately constant, as a consequence of the fact that the p-like states e2, e3, and e4 are nearly degenerate. The addition energy of the ninth electron,  $\Delta_{8,9}^{(e)}$ , is slightly larger, and reflects the single-particle gap between the p-like shell and the next (d-like) shell.

**Hole Addition Energies.** The addition energies of the holes are approximately constant. This is due to the fact that the energy difference between the h1, h2 and the h3, h4 single-particle states is relatively small ( $38 \text{ meV}$  in the  $30.3 \text{ \AA}$  diameter nanocrystal and  $14 \text{ meV}$  in the  $42.2 \text{ \AA}$  diameter nanocrystal) and is comparable with the variations of the direct Coulomb energies  $J_{ij}^{\text{dir}}$  between different hole states. Banin et al.<sup>1</sup> found

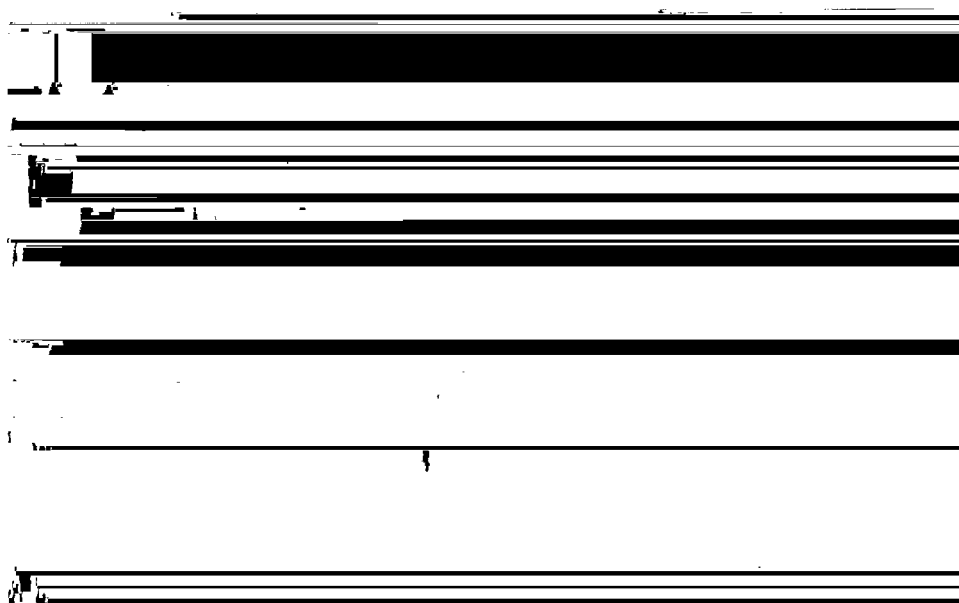


**Figure 3.** (middle panel) Dependence of the electron and hole charging energies on the outside dielectric constant  $\epsilon_{\text{out}}$ . The vertical arrow indicates the value  $\epsilon_{\text{out}} = \epsilon_{\text{in}}$ . The side panels show the calculated charging spectrum in the case  $\epsilon_{\text{out}} = 1$  (left-hand panel) and  $\epsilon_{\text{out}} = 20$  (right-hand panel). The zero of the energy scale corresponds to the highest-energy valence state.

two distinct multiplets in the hole addition spectrum, which they denoted as  $1_{VB}$  and  $2_{VB}$ . They attributed the  $2_{VB}$  multiplet to tunneling of holes into the  $2S_{3/2}$  valence-band level. We find that the  $2S_{3/2}$  level is significantly lower in energy than the  $h1-h4$  levels, so we do not consider hole injection into the  $2S_{3/2}$  level. Our calculations show that charging of the  $h1-h4$  levels produces a rather featureless spectrum, and that the first multiplet in the hole addition spectrum ( $1_{VB}$ ) consists of at least eight nearly equally spaced peaks. The fact that Banin et al.<sup>1</sup> do not observe such a high multiplicity suggests that some of the hole charging peaks may be missing.

**Quasi-Particle and Optical Gap.** As shown in Table 1, the quasi-particle gap  $\epsilon_{gap}^{qp}$  depends strongly on  $\epsilon_{out}$ , while the optical gap  $\epsilon_{gap}^{opt} = \epsilon_{gap}^{qp} - J_{h1,e1}$  does not. This is so because the terms  $(\sum_{h1}^{pol} + \sum_{e1}^{pol})$  and  $J_{h1,e1}^{pol}$  tend to cancel, so  $\epsilon_{gap}^{opt} = (\epsilon_{e1} - \epsilon_{h1}) - J_{h1,e1}^{dir}$ .

Table 1 provides clear predictions for the addition energies and the quasi-particle gap of InAs nanocrystals. To compare with the experimental measurements of Banin et al. (ref 1), in which  $\epsilon_{out}$  is an unknown quantity, we first fit our calculated  $\Delta\phi\phi$